Progress In Electromagnetics Research, PIER 93, 385–401, 2009

A NEW LOOK AT NUMERICAL ANALYSIS OF UNIFORM FIBER BRAGG GRATINGS USING COUPLED MODE THEORY

J.-J. Liau and N.-H. Sun

Department of Electrical Engineering
I-Shou University
Kaohsiung County 84001, Taiwan

S.-C. Lin

Department of Communication Engineering
I-Shou University
Kaohsiung County 84001, Taiwan

R.-Y. Ro, J.-S. Chiang, and C.-L. Pan

Department of Electrical Engineering
I-Shou University
Kaohsiung County 84001, Taiwan

H.-W. Chang

Institute of Electro-optical Engineering and Department of Photonics
National Sun Yat-sen University
Kaohsiung 80424, Taiwan

Abstract—The coupled mode theory (CMT) is used to analyze uniform Fiber Bragg gratings. The multi-mode CMT is expressed as the first-order vector ordinary differential equations (ODEs) with coefficients depending on the propagation distance. We show in this paper that by changing variables, the original couple mode equations (CMEs) can be re-casted as constant coefficient ODEs. The eigenvalue and eigenvector technique (EVVT), the analytic method for solving constant coefficient ODEs, is then applied to solve the coupled mode equations. Furthermore, we also investigate the application of Runge-Kutta method (RKM) to the calculation of the global transfer-function matrix for CMEs. We compare the transmission and the reflection

Corresponding author: H.-W. Chang (hchang@faculty.nsysu.edu.tw).

spectra obtained by EVVT with those by RKM. Both results agree within machine accuracy. Numerical simulations conclude that solving constant coefficient ODEs improves the speed and accuracy of solutions to the original CMEs.

1. INTRODUCTION

Fiber Bragg gratings (FBGs) can couple light from the guided fundamental mode to the counter-propagating guided and cladding modes, and cause a set of loss dips in the transmission spectrum and corresponding peaks in the reflection spectrum [1]. The intensities of these loss peaks are determined by the UV induced index modulation of the core, the length of FBGs, and the overlap between fundamental and cladding modes. Since fiber Bragg gratings have advantages of all-fiber geometry, low insertion loss and low cost etc., they have been used for spectral filtering, dispersion compensation, wavelength tuning, and sensing in optical communication and optoelectronics [1–5].

The characteristics of FBGs have been analyzed by numerous papers [1–3, 6 7]. Erdogan presented the optical properties of fiber Bragg gratings, such as the reflection and dispersion characteristics [1, 2]. Singh et al. developed a simple matrix method to solve a standard Bragg fiber and an unconventional Bragg waveguide [6]. Recently, we presented the numerical approach of the coupled mode theory (CMT) for solving uniform FBGs from a new prospective [7]. The paper outlines the detail of the work including a new derivation of CMT equation and many new numerical results.

Normally, the conventional full wave theory such as the modal analysis method and finite difference frequency domain (FD-FD) methods [8, 9] should be used to analyze the FBG problem. However, due to the tremendous ratio between the total length of the FBG and the wavelength, the straight-forward full wave theory needs lots of storage and computational resources to be viable and practical. Instead, the CMT is widely used to analyze Bragg grating problems when the frequency of interest is near the resonance [1].

The CMT can be expressed as a system of ordinary differential equations (ODEs), which is called the coupled mode equations (CMEs). Note that the CMT is accurate when the periodic perturbation is weak. Since the index variation is very small in FBGs, the CMT is suitable for solving uniform FBGs [1, 2, 7]. By solving CMEs, the transmission and reflection properties of fiber Bragg gratings can be obtained.

To obtain accurate results, the numerical methods of solving

the coupled mode equations play an important role in the analysis. Because the coefficients of CMEs are a function of a propagation distance, CMEs should be solved by numerical methods. Runge-Kutta method is the most commonly used numerical method to solve the system of ordinary differential equations with initial conditions. Forslund and He used RKM to solve the scattering problems for laterally periodic inhomogeneous gratings [10]. The reflection coefficient of a linear dielectric slab embedded between two homogeneous dielectric media is obtained by Hashish by using RKM [11]. Watanabe presented the formulation for arbitrary profiled gratings with anisotropy lossy materials. Outside the grating layer, the transmission matrices of electromagnetic fields is calculated by RKM [12].

As described above, the coupled mode equations are written as a system of first-order ordinary differential equations (ODEs) with the coefficients dependent on propagation distance z-dependent, hereafter named z-dependent coefficient ODEs. On the other hand, we show by changing variables of CMEs, the system of z-dependent coefficient ODEs of CMT can be expressed as a system of ODEs with constant coefficients. It is noted that a first-order constant coefficient ODEs has a rigorous analytic solution using eigenvalue-eigenvector technique (EVVT). By evaluating the eigenvalues and the eigenvectors of the coefficient matrix of the ODEs, the solution of the ODEs can be obtained. Watanabe and Kuto used EVVT to solve the wave propagation in optical waveguides [13].

In this paper, the derivation of constant coefficient ODEs from z-dependent ODE is presented. The EVVT as well as RKM is applied to solve CMT for analyzing uniform FBGs. The formulation of transmission and the reflection coefficients of uniform FBGs are also described. The accuracy of EVVT and RKM are compared in this paper.

2. THE COUPLED MODE THEORY

Fiber gratings are fabricated by exposing an optical fiber to a pattern of ultraviolet intensity. Assume that a time harmonic wave propagates in the z direction as $\exp(i\beta z - i\omega t)$, where β is a propagation constant, and ω is the angular frequency. For simplicity, the refractive index of the fiber grating is described as follows [1]

$$n(r,z) = \begin{cases} n_1 = n_1\sigma_{dc} + n_1\sigma_{dc}m\cos(2\pi z/\Lambda) & r \le r_1 \\ n_2 & r_1 \le r \le r_2 \\ n_3 & r_2 \le r \end{cases} \quad (1)$$

where Λ is the grating period, r_1 and r_2 are the radius of the core and cladding, respectively, and n_1, n_2 and n_3 are the refractive indices of the core, cladding and the surrounding region, respectively. $n_1\sigma_{dc}$ is the dc index change, $n_1\sigma_{dc}m\cos(2\pi z/\Lambda)$ is the ac index change and m is the fringe visibility of the index change. Since the grating is uniform, σ_{dc} is a constant.

The magnitudes of electromagnetic waves for the ith mode in the fiber can be expressed as

$$\vec{U}_i^{+}(r,\phi,z) = A_i(z)\cdot\vec{\Phi}_i(r,\phi)\cdot\exp(i\beta_i z) \tag{2a}$$

$$\vec{U}_i^{-}(r,\phi,z) = B_i(z)\cdot\vec{\Phi}_i(r,\phi)\cdot\exp(-i\beta_i z), \tag{2b}$$

where $\vec{U}_i^{+}(r,\phi,z)$ and $\vec{U}_i^{-}(r,\phi,z)$ are the magnitudes of forward and backward waves with $A_i(z)$ and $B_i(z)$, the corresponding amplitude functions, $\vec{\Phi}_i(r,\phi)$, the two-dimensional 3-D vector field function, and β_i is the propagation constant of the ith mode. Note that without gratings, the coupling between modes can not happen and the amplitude function A_i and B_i remain to be constants. When gratings are fabricated in the core of the fiber, the coupling occurs so that $A_i(z)$ and $B_i(z)$ are functions of the propagation distance.

In the multi-mode coupled mode theory, we consider the interactions between forward and backward mode amplitude functions in an FBG fiber over a grating period $dz = \Lambda$. To the first-order accuracy of dz, the "averaged" effect of mutual coupling among the various waveguide modes can be written as a system of linear ordinary equations below:

$$\frac{dA_0}{dz} = +i\kappa_0 A_0 + i\frac{m}{2}\kappa_0 B_0\exp(-i2\delta_0 z) + i\sum_{\nu}\frac{m}{2}\kappa_v B_v\exp(-i2\delta_v z) \tag{3}$$

$$\frac{dB_0}{dz} = -i\kappa_0 B_0 - i\frac{m}{2}\kappa_0 A_0\exp(+i2\delta_0 z) - i\sum_{\nu}\frac{m}{2}\kappa_v A_v\exp(+i2\delta_v z) \tag{4}$$

$$\frac{dA_v}{dz} = +i\frac{m}{2}\kappa_v B_0\exp(-i2\delta_v z) \quad \text{for } \nu = 1,2,\ldots,n \tag{5}$$

$$\frac{dB_v}{dz} = -i\frac{m}{2}\kappa_v A_0\exp(+i2\delta_v z) \quad \text{for } \nu = 1,2,\ldots,n \tag{6}$$

where $A_0(z)$ is the amplitude for the transverse core mode field traveling to the $+z$ direction, $B_0(z)$ is the amplitude for the transverse core mode field traveling to the $-z$ direction. $A_\nu(z)$ and $B_\nu(z)$ are amplitudes for the νth cladding mode ($v = 1,\ldots,n$). δ is a small-detuning parameter, and κ is the coupling coefficient. The parameters

δ_0, δ_v, κ_0 and κ_v are defined as follows:

$$\delta_0 = \frac{1}{2}\left(2\beta_0 - \frac{2\pi}{\Lambda}\right), \tag{7}$$

$$\delta_v = \frac{1}{2}\left(\beta_0 + \beta_v - \frac{2\pi}{\Lambda}\right), \tag{8}$$

$$\kappa_0 = \frac{\omega\varepsilon_0 n_1^2 \sigma_{dc}}{2}\int_0^{2\pi} d\phi \int_0^{r_1} rdr\left(|E_r^{\mathrm{co}}|^2 + \left|E_\phi^{\mathrm{co}}\right|^2\right), \tag{9}$$

$$\kappa_v = \frac{\omega\varepsilon_0 n_1^2 \sigma_{dc}}{2}\int_0^{2\pi} d\phi \int_0^{r_1} rdr\left(E_r^{\mathrm{cl}} E_r^{\mathrm{co}*} + E_\phi^{\mathrm{cl}} E_\phi^{\mathrm{co}*}\right), \tag{10}$$

where β_0 is the propagation constant of the core mode, β_v is the propagation constant of the vth cladding mode, E_r and E_ϕ are electric fields of transverse components of vector function $\vec{\Phi}(r,\phi)$, in Equations (2a) and (2b). Superscripts co and cl indicate the core mode and the cladding mode. Derivation of Equations (3)–(10), are covered in more detail in reference papers [1, 2, 7] and also in some textbooks [14]. Equations (5) and (6) represent the counter-directional coupling between the core mode and cladding modes. Since we assume that only the core mode is incident into the FBGs, there are no powers of cladding modes in the input end of FBGs. Therefore, the coupling among cladding modes are extremely small and is neglected in the coupled mode equations of Equations (5) and (6). In addition, the co-directional coupling between the core mode and cladding modes are also neglected due to the short period of the grating. For very long period FBG, all co-directional coupling must be included. Ideally, δ_0 should be zero or quite small so every backward reflection from each grating structure will add up coherently.

The CMEs can be expressed as a matrix form:

$$\frac{d\vec{Y}}{dz} = \frac{d}{dz}\begin{bmatrix}\vec{A}\\ \vec{B}\end{bmatrix} = \begin{bmatrix}\mathbf{U_{11}} & \mathbf{U_{12}}\\ \mathbf{U_{21}} & \mathbf{U_{22}}\end{bmatrix}\cdot\begin{bmatrix}\vec{A}\\ \vec{B}\end{bmatrix} = \mathbf{U}(\mathbf{z})\cdot\vec{Y} \tag{11}$$

where $\vec{A} = [A_0, \ldots A_n]^T$ and $\vec{B} = [B_0, \ldots B_n]^T$ are the amplitude vectors propagating in the forward and backward directions, respectively, and the elements of $\vec{A}$ and $\vec{B}$ are A_v and B_v, $v = 0, \ldots, n$ respectively. The amplitude vector $\vec{Y}$ includes $\vec{A}$ and $\vec{B}$. The sub matrices $\mathbf{U}_{11}$ has only one nonzero element $i\kappa_0$, the first entry.

$\mathbf{U}_{12}, \mathbf{U}_{21}$ are given below

$$\begin{aligned}\mathbf{U}_{12} &= \frac{im}{2} \cdot \begin{bmatrix} \kappa_0 e^{-i2\delta_0 z} & \dots & \kappa_n e^{-i2\delta_n z} \\ \vdots & 0 & 0 \\ \kappa_n e^{-i2\delta_n z} & 0 & 0 \end{bmatrix} \\ \mathbf{U}_{21} &= \frac{-im}{2} \cdot \begin{bmatrix} \kappa_0 e^{i2\delta_0 z} & \dots & \kappa_n e^{i2\delta_n z} \\ \vdots & 0 & 0 \\ \kappa_n e^{i2\delta_n z} & 0 & 0 \end{bmatrix}.\end{aligned} \tag{12}$$

Note that due to the structure equivalence between the forward and backward waves, $\mathbf{U}_{21} = -\mathbf{U}_{12}$, $\mathbf{U}_{22} = -\mathbf{U}_{11}$ when z is replaced by $-z$. The fact that these sub-matrices are functions of propagation distance z makes (11) a system of first-order ODEs with z-dependent coefficients.

Next we wish to transform Equation (11) into a system of ODEs with constant coefficients via the change of variables. For an arbitrary general matrix function $\mathbf{U}(z)$, this is not always possible because we can only adjust $2N$ terms in $\vec{A}$ and $\vec{B}$ to remove z-dependence of all $4N^2$ entries in $\mathbf{U}$. Fortunately, by neglecting bi-directional coupling among the cladding modes and co-directional coupling between the core mode and cladding modes, most entries in $\mathbf{U}(z)$ are zeros. Considering the special symmetry of sub-matrices of $\mathbf{U}$, we make the following change of variables and introduce new sets of amplitude functions $\{a_v\}$ and $\{b_v\}$ for the vth mode as,

$$\begin{aligned} a_v &= A_v \exp(i\Delta_\nu z) \\ b_v &= B_v \exp(-i\Delta_v z), \end{aligned} \quad v = 0, 1, 2, \dots, n \tag{13}$$

To determine Δ_ν, we substitute (13) into (11) to annihilate all non-zero coefficients in the exponential terms of the new $\mathbf{U}$ matrix. The detailed derivation is presented in the Appendix A. Using the following perturbed propagation constants:

$$\Delta_v = 2\delta_v - \delta_0, \quad v = 0, 1, 2, \dots, n \tag{14}$$

we can obtain a constant coefficient CMEs for $a_v(z)$ and $b_v(z)$ below:

$$\frac{d\vec{y}}{dz} = \frac{d}{dz} \begin{bmatrix} \vec{a} \\ \vec{b} \end{bmatrix} = \begin{bmatrix} \mathbf{V_{11}} & \mathbf{V_{12}} \\ \mathbf{V_{21}} & \mathbf{V_{22}} \end{bmatrix} \begin{bmatrix} \vec{a} \\ \vec{b} \end{bmatrix} = \mathbf{V} \cdot \vec{y}, \tag{15}$$

where $\vec{a} = [a_0, \ldots a_n]^T$ and $\vec{b} = [b_0, \ldots b_n]^T$ and

$$\begin{aligned}
\mathbf{V}_{11} &= \begin{bmatrix} i(\kappa_0 + \Delta_0) & 0 & \ldots & 0 \\ 0 & i\Delta_1 & \ldots & 0 \\ \vdots & \vdots & \ddots & \vdots \\ 0 & 0 & \ldots & i\Delta_n \end{bmatrix}, \\
\mathbf{V}_{12} &= i\frac{m}{2} \begin{bmatrix} \kappa_0 & \kappa_1 & \ldots & \kappa_n \\ \kappa_1 & 0 & \ldots & 0 \\ \vdots & \vdots & \ddots & \vdots \\ \kappa_n & 0 & \ldots & 0 \end{bmatrix} \\
\mathbf{V}_{21} &= -\mathbf{V}_{12}, \quad \mathbf{V}_{22} = -\mathbf{V}_{11}.
\end{aligned} \tag{16}$$

The amplitude vector $\vec{y}$ includes forward propagating vector $\vec{a}$ and backward propagating vector $\vec{b}$. Since all elements of $\mathbf{V}$ in (16) are constants, the analytical solution of the coupled mode Equation (15) can be obtained by the eigenvalue eigenvector technique. To our knowledge Equations (15), (16) have never been published in the literature. The complete mathematical description of CMT requires the following boundary conditions to be satisfied

$$\vec{a}_0 \stackrel{\Delta}{=} \vec{a}(0) = [1 \;\; 0 \;\; \ldots \;\; 0]^T, \quad \vec{b}_L \stackrel{\Delta}{=} \vec{b}(L) = [1 \;\; 0 \;\; \ldots \;\; 0]^T. \tag{17}$$

The reflection and transmission coefficient vectors are given by

$$\vec{r}_0 = [r_0 \;\; r_1 \;\; \ldots \;\; r_n]^T = \vec{b}(0), \quad \vec{t}_L = [t_0 \;\; t_1 \;\; \ldots \;\; t_n]^T = \vec{a}(L) \tag{18}$$

3. EIGENVALUE-EIGENVECTOR TECHNIQUE

The constant coefficient ODEs can be analytically solved by eigenvalue-eigenvector technique (EVVT). Using EVVT, the rigorous solution of (15) can be expressed as

$$\begin{aligned}
\vec{y}(z) &= \sum_{i=1}^{2n} c_i \cdot \vec{p}_i \cdot e^{\lambda_i z} \\
&= \begin{bmatrix} p_{11}e^{\lambda_1 z} & \ldots & p_{1,2n}e^{\lambda_{2n} z} \\ \vdots & \ddots & \vdots \\ p_{2n,1}e^{\lambda_1 z} & \ldots & p_{2n,2n}e^{\lambda_{2n} z} \end{bmatrix} \begin{bmatrix} c_1 \\ c_2 \\ \vdots \\ c_{2n} \end{bmatrix} = \mathbf{Q}(\mathbf{z}) \cdot \vec{c}
\end{aligned} \tag{19}$$

where $\lambda_i, \vec{p}_i = [\; p_{1,i}, \;\; \ldots \;\; p_{2n,i} \;]^T$ is the ith eigenvalue and its corresponding eigenvector of matrix $\mathbf{V}$ in (15). $\vec{c}$ is the unknown

eigenfunction coefficient vector which is determined by the boundary conditions. From (19), the transfer-function matrix $\mathbf{G}$ that connects $\vec{y}(0)$ to $\vec{y}(L)$ is given by

$$\vec{y}(L) = \mathbf{G} \cdot \vec{y}(0), \quad \mathbf{G} = \mathbf{Q}(L) \cdot \mathbf{Q}(0)^{-1} \tag{20}$$

$$\vec{y}(L) = \begin{bmatrix} \vec{a}_L \\ \vec{b}_L \end{bmatrix}, \quad \vec{y}(0) = \begin{bmatrix} \vec{a}_0 \\ \vec{b}_0 \end{bmatrix}. \tag{21}$$

By definition, reflection and transmission vectors ($\vec{r}_0$ and $\vec{t}_L$) are $\vec{a}_0$ and $\vec{b}_L$ in (21). We obtain

$$\begin{bmatrix} \vec{t}_L \\ \vec{b}_L \end{bmatrix} = \begin{bmatrix} \mathbf{G}_{11} & \mathbf{G}_{12} \\ \mathbf{G}_{21} & \mathbf{G}_{22} \end{bmatrix} \cdot \begin{bmatrix} \vec{a}_0 \\ \vec{r}_0 \end{bmatrix}, \quad \mathbf{G} = \begin{bmatrix} \mathbf{G}_{11} & \mathbf{G}_{12} \\ \mathbf{G}_{21} & \mathbf{G}_{22} \end{bmatrix}. \tag{22}$$

By rearranging (22), the equation and solutions of $\vec{r}_0$ and $\vec{t}_L$ can be written as

$$\begin{aligned} \vec{r}_0 &= \mathbf{G}_{22}^{-1} \cdot \left(\vec{b}_L - \mathbf{G}_{21} \cdot \vec{a}_0 \right), \\ \vec{t}_L &= \left(\mathbf{G}_{11} - \mathbf{G}_{12} \cdot \mathbf{G}_{22}^{-1} \cdot \mathbf{G}_{21} \right) \cdot \vec{a}_0 + \mathbf{G_{12}} \cdot \mathbf{G}_{22}^{-1} \cdot \vec{b}_L. \end{aligned} \tag{23}$$

4. RUNGE-KUTTA METHOD

Runge-Kutta method (RKM) is one of the most commonly used numerical methods to solve an initial value problem (IVP) described by a system of ordinary differential equations. RKM is the ideal method for solving system of ODEs with smoothly varying coefficients.

At the first application of RKM to advance the vector functions $\vec{Y}(0)$ in (11) to the next step $\vec{Y}(dz)$, we find that part of the initial conditions are missing. It is because we do not know what $\vec{r}_0$ is. To make RKM work, we must update $\vec{Y}(z)$ vectors due to all possible initial conditions. In other words, we need to compute the transfer-function matrix that will take us from any arbitrary initial vector $\vec{Y}(0)$ to $\vec{Y}(dz)$ and eventually to $\vec{Y}(L)$. We begin RKM process by first dividing the grating region $0 < z < L$ into m equally spaced sections, each with a length $h = L/m$. The centered position of the ith section is $z_i = (i - 1/2) \cdot h$ for $i = 1, \ldots, m$. When we apply the fourth-order RKM method, the local transfer-function $\mathbf{R}_i$ is written as

$$\mathbf{R}_i = \mathbf{I} + \left(\mathbf{K}_{1i} + 2\mathbf{K}_{2i} + 2\mathbf{K}_{3i} + \mathbf{K}_{4i} \right) / 6, \tag{24}$$

where matrices $\mathbf{K}_{1i}$, $\mathbf{K}_{2i}$, $\mathbf{K}_{3i}$ and $\mathbf{K}_{4i}$ are intermediate Runge-Kutta calculations given by

$$\begin{aligned}
\mathbf{K}_{1i} &= h \cdot \mathbf{U}(z = i \cdot h - h) \\
\mathbf{K}_{2i} &= h \cdot \mathbf{U}(z = i \cdot h - h/2) \cdot (\mathbf{I} + \mathbf{K}_{1i}/2) \\
\mathbf{K}_{3i} &= h \cdot \mathbf{U}(z = i \cdot h - h/2) \cdot (\mathbf{I} + \mathbf{K}_{2i}/2) \\
\mathbf{K}_{4i} &= h \cdot \mathbf{U}(z = i \cdot h) \cdot (\mathbf{I} + \mathbf{K}_{3i}/2).
\end{aligned} \tag{25}$$

Each $\mathbf{R}_i$ connects the two amplitude vectors at the two ends of the section as

$$\vec{Y}(ih) = \mathbf{R}_i \cdot \vec{Y}((i-1)h). \tag{26}$$

Like Equation (20), these transfer-function matrices $\mathbf{R}_i$, $i = 1, \ldots, m$, help to connect the amplitude vector $\vec{Y}$ at $z = L$ with $\vec{Y}$ at $z = 0$ in the following way:

$$\begin{aligned}
\vec{Y}(L) &= \mathbf{U}(mh) = \mathbf{R}_m \cdot \vec{Y}((m-1)h) \\
&= \mathbf{R}_m \cdot \mathbf{R}_{m-1} \ldots \mathbf{R}_1 \cdot \vec{Y}(0) = \mathbf{G}_{\mathrm{RKM1}} \cdot \vec{Y}(0).
\end{aligned} \tag{27}$$

Matrix $\mathbf{G}_{\mathrm{RKM1}}$ is the global transfer matrix computed by Runge-Kutta method for solving z-dependent coefficient CMEs (11).

The RKM is also used to solve the constant coefficient CMEs (15). Since V in (16) is a constant matrix for all positions z_i of the gratings, all the local transfer-function matrix are the same. The resulting local transfer-function matrix $\mathbf{R}$ is written as

$$\mathbf{R} = \mathbf{I} + (\mathbf{K}_1 + 2\mathbf{K}_2 + 2\mathbf{K}_3 + \mathbf{K}_4)/6, \tag{28}$$

where $\mathbf{K}_1, \ldots \mathbf{K}_4$ are like those in (25) except that $\mathbf{U}$ is replaced by $\mathbf{V}$. We have from (27)

$$\vec{y}(L) = \mathbf{R}^m \vec{y}(0) = \mathbf{G}_{\mathrm{RKM2}} \vec{y}(0). \tag{29}$$

$\mathbf{G}_{\mathrm{RKM2}}$ is the global transfer-function matrix computed by Runge-Kutta method for solving constant coefficient CMEs (15). Once $\mathbf{G}_{\mathrm{RKM}}$ matrices are computed, we then apply Equations (23a) and (23b) to compute transmission and reflection amplitude vectors. Thus, the solutions to CMEs can be obtained by using RKM.

The transmission and reflection efficiencies of the core mode can be expressed as

$$T = \frac{|A_0(L)|^2}{|A_0(0)|^2} = |A_0(L)|^2, \quad R = \frac{|B_0(0)|^2}{|A_0(0)|^2} = |B_0(0)|^2. \tag{30}$$

where $A_0(L)$ and $B_0(0)$ are the first element of $\vec{A}(L)$ and $\vec{B}(0)$, respectively.

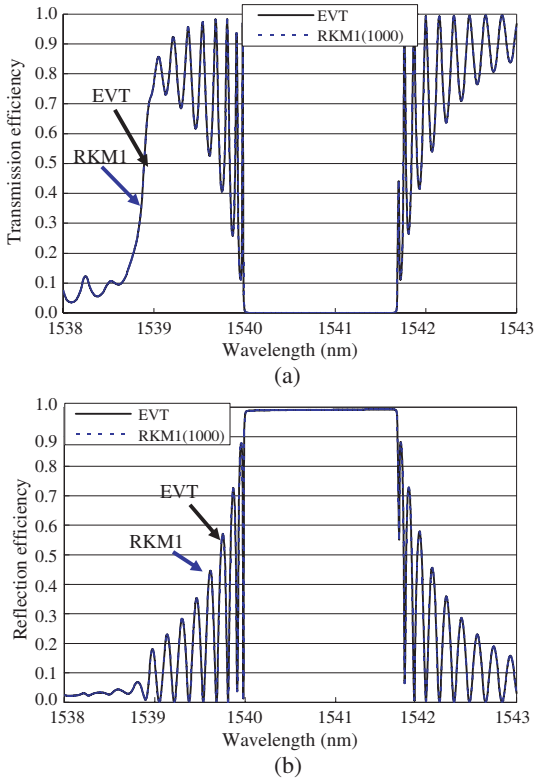

Figure 1. (a) The transmission spectrum of uniform FBGs using EVVT and RKM. The step number of RKM is 1000. (b) The reflection spectrum of uniform FBGs using EVVT and RKM. The step number of RKM is 1000.

5. RESULTS AND DISCUSSION

Assume that an FBG is made of a step index single-mode fiber. The radius of core and cladding of the fiber are $r_1 = 2.5\,\mu\text{m}$ and $r_2 = 62.5\,\mu\text{m}$, respectively. The refractive indices of the core, cladding and surrounding region are $n_1 = 1.458$, $n_2 = 1.45$ and $n_3 = 1$, respectively. The grating period is $\Lambda = 0.53\,\mu\text{m}$, the induced-index change $n_1\sigma_{dc}$ is 2.8×10^{-3}, and the total length of the FBG is $L = 4\,\text{mm}$. The parameters of the FBGs used in our calculation are from [2]. We consider a total of twenty-five modes in all of our numerical work.

Figures 1(a) and 1(b) show the transmission spectrum and reflection spectrum, respectively, by using RKM1 and EVVT. The solid

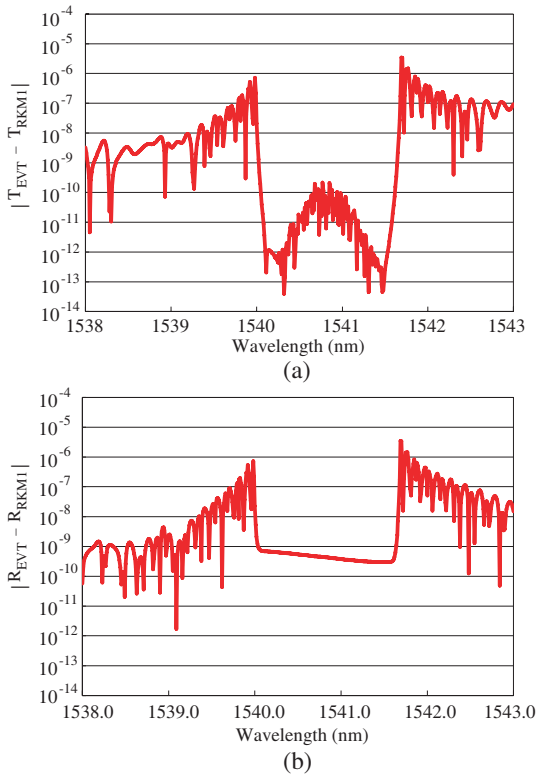

Figure 2. (a) The difference of the transmission efficiencies between the EVVT and RKM1. (b) The difference of the reflection efficiencies between the EVVT and RKM1.

lines in Figs. 1(a) and 1(b) are the results of Equation (15) by EVVT, while the dash line indicates the solutions of Equation (11) by RKM1. The grating length is divided by 1000 points in our calculation.

As shown in Fig. 1, the transmission and the reflection spectrum in the resonant region of first Bragg are symmetric, where the 3 dB resonant region is from 1539.98 nm to 1541.70 nm, and the 3 dB bandwidth is 1.72 nm. The central wavelength of the resonance is 1540.84 nm. The sidelobe suppressions on two sides of the resonance are about 11% corresponding to the wavelengths of 1539.96 nm and 1541.72 nm. Note that the cladding mode coupling can be found in Fig. 1. At the cladding mode coupling region, the core mode transfers the power to contra-propagating cladding modes, but not the core mode. Therefore, both the transmitted and reflected powers of the core mode are decreased. In Fig. 1, the cladding mode coupling occurs

at the wavelength less than 1539 nm, where the transmission efficiencies decrease to 10%, and the reflection efficiencies remain 10%.

The differences of the transmission efficiency and the reflection efficiency between RKM1 and EVVT in Fig. 2 are shown in Figs. 2(a) and 2(b), respectively. As shown in Fig. 2, in the resonant region the differences of transmissivity and reflectivity for the two methods are relatively small (less than 10^{-9}) compared with those out of the resonant region. It is because at resonance, the CME satisfies the phase-matching condition, i.e., the small-detuning parameter of the core mode δ_0 in (7) is approaching to zero. The coefficients of A_0 and B_0 in (11) are near constants. Therefore, A_0 and B_0 can be calculated by numerical methods with small numerical error. On the other hand, off the resonant region, the maximum differences between EVVT and RKM1 for both the transmission and reflection efficiencies occur at the same wavelength of 1541.69 nm (in the right edge of the resonant region in Fig. 2), and is about 3.4×10^{-6}. Note that off resonance, the coefficients of A_0 and B_0 in (11) are a function of the exponential form with a variable of a propagation distance. The numerical error of the z-dependent coefficient ODEs oscillates with respect to the wavelength.

Although the EVVT is a rigorous method to solve constant coefficient ODEs, the error of EVVT is caused by the numerical error of eigenvalues and eigenvectors. Since eigenvalues and eigenvectors can be correctly obtained by several numerical methods or software, the EVVT can provide more accurate results than RKM. Therefore, we define the error as the differences of calculated results between RKM and EVVT. Figs. 3(a) and 3(b) show the error of transmission and reflectivity, respectively, as a function of a step number of RKM at the wavelength of 1541.69 nm. The wavelength of 1541.69 nm is chosen because it is the maximum error in Figs. 2(a) and 2(b). Both errors of RKM1 and RKM2 are shown in Figs. 3(a) and 3(b), where RKM1 indicates solutions of z-dependent coefficient ODEs (11) solved by RKM, and RKM2 denotes solutions of constant coefficient ODEs (15) solved by RKM. As shown in Figs. 3(a) and 3(b), the calculated results by RKM1 and RKM2 approach the results calculated by EVVT with increased step numbers.

Figure 3(a) shows that RKM1 presents the same convergent rate with increased step numbers. When the step number is 1000, the error of RKM1 is 3.4×10^{-6}, while the error is 3.4×10^{-10} for 10000 steps of RKM1. The result demonstrates that if the step size h is decreased by 10^{-1}, the local truncation error decreases to 10^{-4} times. It means that the rate of convergence for RKM1, or the local truncation error of RKM1, is $O(h^{-4})$, where $O(h^{-4})$ denotes the order of the local truncation error of h^{-4} (please see Appendix B) [15]. Our calculated

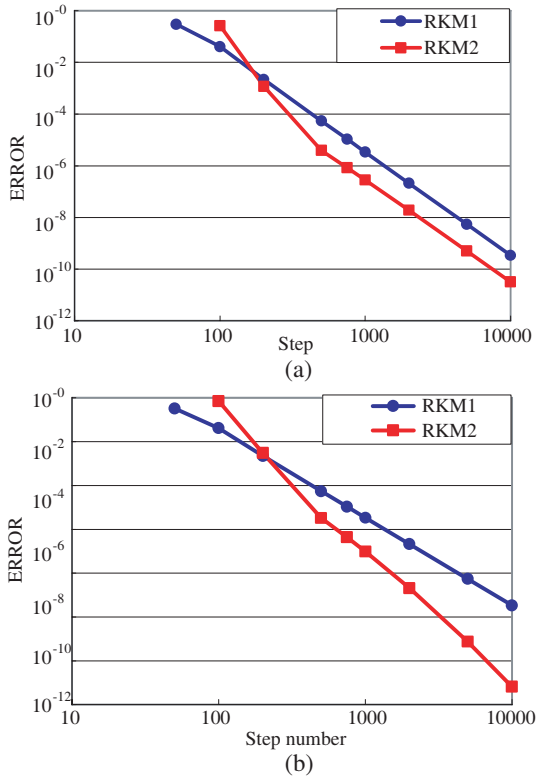

Figure 3. (a) The error of transmissivity by RKM1 and RKM2 as a function of step number at wavelength of 1541.69 nm. (b) The error of reflectivity by RKM1 and RKM2 as a function of step number at wavelength of 1541.69 nm.

truncation error of $O(h^{-4})$ is the same as theoretical results of the fourth-order RKM. For RKM2 in Fig. 3(a), we can find that two convergent rates correspond to the step number. When the step number is less than 500, the convergent rate of RKM2 is $O(h^{-7})$. When the step number is greater than 500, the two curves of RKM1 and RKM2 are almost parallel. It means that the two slopes represent the same truncation errors of $O(h^{-4})$. Therefore, even though the error of RKM2 is lager than that of RKM1 when the step number is 100, RKM2 is more accurate at the step number of 10000. The errors of RKM1 and RKM2 at the step number of 10000 are 3.4×10^{-10} and 3.2×10^{-11}, respectively.

Similar to Fig. 3(a), the local truncation error (or the convergent

rate) of RKM1 for reflectivity is $O(h^{-4})$ in Fig. 3(b) and is the same as that for transmissivity. Two rates of the convergence for RKM2 are found in Fig. 3(b) as well. When the step number is less than 500, the convergent rate of RKM2 is $O(h^{-7})$ while it is $O(h^{-8})$ when the step number is greater than 500. Note that the convergent rate of RKM2 for the reflectivity is faster than that for the transmission efficiency. The error of RKM2 in Fig. 3(b) is 10^{-4} times of that of RKM1 when the step number is 10000, where the errors of the 10000-step for RKM1 and RKM2 are 3.4×10^{-10} and 6.7×10^{-14}, respectively. Compare Fig. 3(a) with Fig. 3(b). The errors for RKM1 are similar. But RKM2 can obtain more accurate reflectivity than tranmsissivity. Also, at the step number of 200, both RKM1 and RKM2 have similar truncation errors of reflection and transmission.

6. CONCLUSIONS

The coupled mode theory applied to the analysis of uniform FBGs is reinvestigated with the fundamental guided mode and a total of 24 cladding modes. By changing variables and taking the advantage that most entries in the coefficient matrix are zero, we derive the system of constant coefficient ODEs from the system of z-dependent coefficient ODEs. The constant coefficient ODEs is solved by the standard eigenvalue eigenvector technique and we obtained transmission and reflection coefficient vectors. We also show how the simple but effective Runge-Kutta method can be applied to compute the global transfer-function matrix described by the z-dependent coefficient ODEs (labeled as RKM1). Since constant coefficient ODEs can be solved "exactly" by the rigorous EVVT, their results are used as references. RKM, on the other hand, has the advantage of being simpler than the EVVT.

For comparison, using the constant coefficient ODEs, the transmission and reflection amplitude spectra of uniform FBGs were computed by both EVVT and RKM (labeled as RKM2). Both RKM1 and RKM2 results approach those by EVVT when we increased the number of steps m. The calculated results show that RKM2 is more accurate than RKM1. In some cases, using equal number of steps, the error of RKM1 is 10^4 times of that of RKM2. In addition, we observed an $O(h^{-7})$ convergent rate in RKM2 which is much better than the expected $O(h^{-4})$ convergent rate from RKM1.

ACKNOWLEDGMENT

The authors would like to thank Professor Yean-Woei Kiang, Department of Electrical Engineering, National Taiwan University for suggesting to us a way to convert the original CMEs into a constant coefficient ODEs. We are also grateful to the support of the National Science Council of the Republic of China under the contracts NSC97-972221-E-110016 and NSC96-2221-E-214-023-MY3. This work is also supported by the Ministry of Education, Taiwan, under the Aim-for-the-Top University Plan.

APPENDIX A. DETAIL DERIVATION OF (15) AND (16)

We start with the definitions:

$$\begin{aligned} \vec{a}(z) &= e^{i\mathbf{\Delta}z}\vec{A}(z), \quad \vec{b}(z) = e^{-i\mathbf{\Delta}z}\vec{B}(z), \\ \vec{A}(z) &= e^{-i\mathbf{\Delta}z}\vec{a}, \quad \vec{B}(z) = e^{i\mathbf{\Delta}z}\vec{b}(z). \end{aligned} \tag{A1}$$

where the diagonal matrix $\mathbf{\Delta}$ is made of entries $\Delta_0, \ldots, \Delta_n$. Taking derivative of (A1), we get

$$\begin{aligned} \frac{d\vec{a}}{dz} &= \frac{d}{dz}\left(e^{i\mathbf{\Delta}z}\vec{A}\right) = i\mathbf{\Delta}\vec{a} + e^{i\mathbf{\Delta}z}\frac{d\vec{A}}{dz}, \\ \frac{d\vec{b}}{dz} &= \frac{d}{dz}\left(e^{-i\mathbf{\Delta}z}\vec{B}\right) = -i\mathbf{\Delta}\vec{b} + e^{-i\mathbf{\Delta}z}\frac{d\vec{B}}{dz}. \end{aligned} \tag{A2}$$

Substituting (A1) and (11) into (A2), we get

$$\begin{aligned} \frac{d\vec{a}}{dz} &= i\mathbf{\Delta}\vec{a} + e^{i\mathbf{\Delta}z}\mathbf{U}_{11}e^{-i\mathbf{\Delta}z}\vec{a} + e^{i\mathbf{\Delta}z}\mathbf{U}_{12}e^{i\mathbf{\Delta}z}\vec{b} = \mathbf{V}_{11}\vec{a} + \mathbf{V}_{12}\vec{b}, \\ \frac{d\vec{b}}{dz} &= -i\mathbf{\Delta}\vec{b} + e^{-i\mathbf{\Delta}z}\mathbf{U}_{21}e^{-i\mathbf{\Delta}z}\vec{a} - e^{-i\mathbf{\Delta}z}\mathbf{U}_{22}e^{i\mathbf{\Delta}z}\vec{b} = \mathbf{V}_{21}\vec{a} + \mathbf{V}_{22}\vec{b}. \end{aligned} \tag{A3}$$

$$\mathbf{V}_{12} = e^{i\mathbf{\Delta}z}\mathbf{U}_{12}e^{i\mathbf{\Delta}z} = i\frac{m}{2}\cdot \begin{bmatrix} \kappa_0 e^{iz(2\Delta_0-\delta_0)} & \kappa_1 e^{iz(\Delta_0+\Delta_1-2\delta_1)} & \cdots & \kappa_n e^{iz(\Delta_0+\Delta_n-2\delta_n)} \\ \kappa_1 e^{iz(\Delta_0+\Delta_1-2\delta_1)} & 0 & \cdots & 0 \\ \vdots & \vdots & \ddots & \vdots \\ \kappa_n e^{iz(\Delta_0+\Delta_n-2\delta_n)} & 0 & \cdots & 0 \end{bmatrix}, \tag{A4}$$

$$\mathbf{V}_{21} = e^{-i\mathbf{\Delta}z}\mathbf{U}_{21}e^{-i\mathbf{\Delta}z} = -i\frac{m}{2}\cdot \begin{bmatrix} \kappa_0 e^{-iz(2\Delta_0-\delta_0)} & \kappa_1 e^{-iz(\Delta_0+\Delta_1-2\delta_1)} & \dots & \kappa_n e^{-iz(\Delta_0+\Delta_n-2\delta_n)} \\ \kappa_1 e^{-iz(\Delta_0+\Delta_1-2\delta_1)} & 0 & \dots & 0 \\ \vdots & \vdots & \ddots & \vdots \\ \kappa_n e^{-iz(\Delta_0+\Delta_n-2\delta_n)} & 0 & \dots & 0 \end{bmatrix}. \quad \text{(A5)}$$

$\mathbf{V}_{12}, \mathbf{V}_{21}$ become constant matrices if $e^{iz(\Delta_0+\Delta_m-2\delta_m)} = 1$ for $m = 0, 1, \dots, n$. We arrive at the following equations:

$$\Delta_m = 2\delta_m - \delta_0 \quad m = 0, 1, \dots, n \quad \text{(A6)}$$

Finally, from (A3) we get, by inspection

$$\begin{aligned} \mathbf{V}_{11} &= e^{i\mathbf{\Delta}z}\mathbf{U}_{11}e^{-i\mathbf{\Delta}z} = \mathbf{U}_{11}, \\ \mathbf{V}_{22} &= e^{-i\mathbf{\Delta}z}\mathbf{U}_{22}e^{i\mathbf{\Delta}z} = \mathbf{U}_{22}. \end{aligned} \quad \text{(A7)}$$

APPENDIX B. DEFINITION OF $O(\beta_n)$

The definition of $O(\beta_n)$ refers from [15]. Suppose $\{\beta_n\}_{n=1}^{\infty}$ is a sequence known to converge to zero, and $\{\alpha_n\}_{n=1}^{\infty}$ converges to a number α. If a positive constant K exists with

$$|\alpha_n - \alpha| \leq K|\beta_n| \text{ for large } n,$$

then $\{\alpha_n\}_{n=1}^{\infty}$ converges to α with rate of convergence $O(\beta_n)$.

REFERENCES

1. Erdogan, T., "Fiber grating spectra," *J. Lightwave Technol.*, Vol. 15, 1277–1294, 1997.
2. Erdogan, T., "Cladding-mode resonances in short- and long-period fiber grating filters," *J. Opt. Soc. Am. A*, Vol. 14, 1760–1773, 1997.
3. Prokopovich, D. V., A. V. Popov, and A. V. Vinogradov, "Analytical and numerical aspects of Bragg fiber design," *Progress In Electromagnetics Research B*, Vol. 6, 361–379, 2008.
4. He, M., J. Jiang, J. Han, and T. Liu, "An experiment research on extend the range of fiber Bragg grating sensor for strain measurement based on CWDM," *Progress In Electromagnetics Research Letters*, Vol. 6, 115–121, 2009.

5. Moghimi, M. J., H. Ghafoori-Fard, and A. Rostami, "Analysis and design of all-optical switching in apodized and chirped Bragg gratings," *Progress In Electromagnetics Research B*, Vol. 8, 87–102, 2008.
6. Singh, V., Y. Prajapati, and J. P. Saini, "Modal analysis and dispersion curves of a new unconventional Bragg waveguide using a very simple method," *Progress In Electromagnetics Research*, PIER 64, 191–204, 2006.
7. Liau, J.-J., N.-H. Sun, R.-Y. Ro, P.-J. Chiang, and S.-C. Lin, "Numerical approaches for solving coupled mode theory — Part I: Uniform fiber Bragg gratings," *Progress In Electromagnetics Research Symposium (PIERS)*, 2A6-3, Hangzhou, China, 2008.
8. Chang, H.-W. and W.-C. Cheng, "Analysis of dielectric waveguide termination with tilted facets by analytic continuity method," *Journal of Electromagnetic Waves and Applications*, Vol. 21, 1621–1630, 2007.
9. Sha, W., X. L. Wu, Z. X. Huang, and M. S. Chen, "Waveguide simulation suing the high-order symplectic finite-difference time-domain scheme," *Progress In Electromagnetics Research B*, Vol. 13, 237–256, 2009.
10. Forslund, O. and S. He, "Electromagnetic scattering from an inhomogeneous grating using a wave-splitting approach," *Progress In Electromagnetics Research*, PIER 19, 147–171, 1998.
11. Hashish, E. A., "Forward and inverse scattering from an inhomogeneous dielectric slab," *Journal of Electromagnetic Waves and Applications*, Vol. 17, 719–736, 2003.
12. Watanabe, K., "Fast converging and widely applicable formulation of the differential theory for anisotropic gratings," *Progress In Electromagnetics Research*, PIER 48, 279–299, 2004.
13. Watanabe, K. and K. Kuto, "Numerical analysis of optical waveguides based on periodic Fourier transform," *Progress In Electromagnetics Research*, PIER 64, 1–21, 2006.
14. Saleh, B. E. A. and M. C. Teich, *Fundamental of Photonics*, John Wiley & Son, New York, 1991.
15. Burden, R. L. and J. D. Faires, *Numerical Analysis*, Brooks/Cole, Pacific Grove, CA, 2001.